Journal of the Korean Chemical Society
2023, *Vol. 67, No. 5*
Printed in the Republic of Korea
https://doi.org/10.5012/jkcs.2023.67.5.333

Monte Carlo Simulations and DFT Studies of the Structural Properties of Silicon Oxide Clusters Reacting with a Water Molecule

Jisu Lee† and Gyun-Tack Bae*
Department of Chemistry Education, Chungbuk National University, Cheongju 28644, Korea.
**E-mail: gtbae@chungbuk.ac.kr*
†*Chungbuk National University Middle School, Cheongju 28402, Korea.*
(Received August 10, 2023; Accepted August 31, 2023)

ABSTRACT. In this study, the H_2O reaction with SiO clusters was investigated using *ab initio* Monte Carlo simulations and density functional theory calculations. Three chemistry models, PBE1/DGDZVP (Model **1**), PBE1/DGDZVP (Si atom), and aug-cc-pVDZ (O and H atoms), (Model **2**) and PBE1/aug-cc-pVDZ (Model **3**), were used. The average bond lengths, as well as the relative and reaction energies, were calculated using Models **1**, **2**, and **3**. The average bond lengths of Si-O and O-H are 1.67-1.75 Å and 0.96-0.97 Å, respectively, using Models **1**, **2**, and **3**. The most stable structures were formed by the H transfer from an H_2O molecule except for **Si_3O_3-H_2O-1** cluster. The Si_3O_3 cluster with H_2O exhibited the lowest reaction energy. In addition, the Bader charge distributions of the Si_nO_n and $(SiO)_n$-H_2O clusters with n = 1-7 were calculated using Model **1**. We determined that the reaction sites between H_2O and the SiO clusters possessed the highest fraction of electrons.

Key words: Monte carlo simulations, Density functional theory, Silicon oxide clusters, Bader charge distribution, Water reaction

INTRODUCTION

SiO clusters have been used in numerous fields, such as optical communications,[1,2] thin film technology,[3] electronics,[4] and biomedical applications.[5] Experimentally, the oxygen etching of cationic and anionic Si clusters has been investigated,[6] as well as silicon monoxide using TOF-MS[7] and Si film with oxygen using synchrotron radiation Si 1s photoemission spectroscopy.[8] Theoretically,[9-15] the equilibrium geometries, binding energies, and ionization potentials, as well as the vertical and adiabatic electron affinities of Si_nO_m clusters ($n \leq 6$, $m \leq 8$), have been examined using density functional theory (DFT) calculations.[10] A systematic study on the structure and stability of SiO_n (n = 1-4), Si_2O_n (n = 1-5), Si_3O_n (n = 1-7), Si_4O_n (n = 1-9), and Si_5O_n (n = 1-11) clusters was reported using *ab initio* molecular dynamics, Monte Carlo (MC), and DFT calculations.[12]

Herein, research was conducted to determine the best chemistry model for small SiO clusters.[14] Particularly, three chemistry models were investigated: PBE1/DGDZVP (Model **1**), PBE1/DGDZVP (Si atom) and aug-cc-pVDZ (O and H atoms) (Model **2**), and PBE1/aug-cc-pVDZ (Model **3**). DGDZVP is double ζ + valence polarization basis set equivalent one used DGauss[16,17] and aug-cc-pVDZ is augmented versions of Dunning's correlation-consistent polarized valence-only basis set.[18-22] The aug-cc-pVDZ basis set is extremely useful in the investigation of metal oxide clusters.[23,24] Model **1** was in good agreement with the experimental data and is computationally inexpensive. Using Model **1**, neutral, cationic, and anionic SiO clusters, Si_nO_n (n = 1-7), were investigated using *ab initio* MC simulations and DFT calculations.[15] Particularly, the H_2O reaction with optimized SiO clusters was investigated using *ab initio* MC simulations and DFT calculations.

METHODS

All geometries of the $(SiO)_n$-H_2O clusters with n = 1-7 were optimized using the Gaussian 09 program.[25] The initial geometries were created by adding an H_2O molecule to multiple sites of the optimized SiO clusters. For example, to construct the initial SiO-H_2O structures, H_2O molecules were attached to the optimized SiO cluster at multiple sites. Therefore, seven initial geometries of the SiO-H_2O clusters were created, and *ab initio* MC simulations were performed. The number of the initial geometries of the Si_2O_2-H_2O, Si_3O_3-H_2O, Si_4O_4-H_2O, Si_5O_5-H_2O, Si_6O_6-H_2O, and Si_7O_7-H_2O clusters were 48, 80, 85, 20, 57, and 65, respectively. *Ab initio* MC simulations using the Gaussian 09 program were home grown scripts. The temperature was decreased from 2000 to 300 K for up to 300 MC steps. *Ab initio* MC simulations have been explained in detail in previous investigations.[15,26-28]

***Table* 1.** Bader charge distributions of the neutral Si_nO_n cluster with n = 1-7 using Model **1**

	qSi(atom number)			qO(atom number)		
SiO	1.91(1)			-1.89(2)		
Si_2O_2	2.09(1)	2.09(2)		-2.02(3)	-2.13(4)	
Si_3O_3	2.10(1)	2.10(2)	2.10(3)	-2.07(4)	-2.05(5)	-2.09(6)
Si_4O_4	2.13(1)	2.13(2)	2.13(3)	-2.14(5)	-2.25(6)	-2.21(7)
	2.13(4)			-2.26(8)		
Si_5O_5	2.13(1)	2.10(2)	1.88(3)	-2.00(6)	-2.10(7)	-1.97(8)
	2.11(4)	2.07(5)		-2.08(9)	-2.24(10)	
Si_6O_6	2.13(1)	2.10(2)	1.90(3)	-2.10(7)	-2.13(8)	-2.06(9)
	2.13(4)	2.10(5)	2.13(6)	-2.20(10)	-2.08(11)	-2.15(12)
Si_7O_7	2.09(1)	2.13(2)	1.94(3)	-2.03(8)	-2.06(9)	-2.12(10)
	2.60(4)	2.15(5)	1.53(6)	-2.09(11)	-2.08(12)	-2.09(13)
	2.15(7)			-2.09(14)		

Following *ab initio* MC simulations, DFT calculations were performed to determine the stable $(SiO)_n$-H_2O structures with n = 1-7. In the DFT calculations, three chemistry models (Models **1**, **2**, and **3**) were used. Model **1** was in good agreement with the experimental data for the SiO clusters.[14] The Bader charge distributions[29] were calculated to determine the reaction site between the SiO clusters and H_2O. The Bader charge distributions of the SiO clusters and $(SiO)_n$-H_2O clusters with n = 1-7 are listed in *Tables* 1 and 4, respectively.

RESULTS AND DISCUSSION

Neutral and charged SiO clusters using *ab initio* MC and DFT (Model **1**), and the optimized neutral SiO clusters are shown in *Fig.* 1.[15]

Among the SiO-H_2O clusters, only two types of structures were simulated, and the optimized SiO-H_2O clusters using Model **1** are presented in *Fig.* 2. All $(SiO)_n$-H_2O clusters with n = 1-7 were optimized using Models **1**, **2**, and **3**. **SiO-H_2O-1** cluster was the most stable structure, in which the H atom of the H_2O molecule was transferred to the O atom of the optimized SiO cluster, and the OH bond was attached to the Si(1) atom. The average bond lengths of Si-O and O-H in the $(SiO)_n$-H_2O clusters using Models **1**, **2**, and **3** are listed in *Table* 2. The average bond lengths

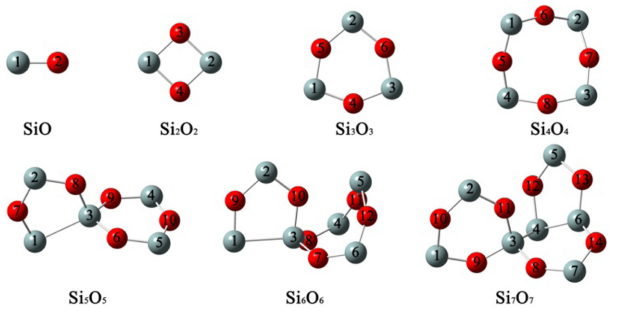

***Figure* 1.** Optimized SiO clusters, $(SiO)_n$ (n = 1-7), using the PBE/DGDZVP chemistry model. Si and O atoms are denoted by gray and red spheres, respectively.[15]

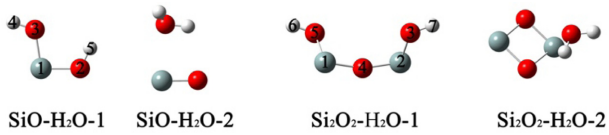

***Figure* 2.** Optimized structures of the SiO-H_2O and Si_2O_2-H_2O clusters using Model **1**. Si, O, and H atoms are denoted by gray, red, and white spheres, respectively.

***Table* 2.** Average bond lengths (Å) of the Si-O and O-H bonds in the most stable $(SiO)_n$-H_2O clusters in Models **1**, **2**, and **3**

Clusters		Model **1**	Model **2**	Model **3**
SiO-H_2O-1	Si-O	1.67	1.68	1.68
	O-H	0.97	0.97	0.97
Si_2O_2-H_2O-1	Si-O	1.67	1.67	1.67
	O-H	0.97	0.96	0.96
Si_3O_3-H_2O-1	Si-O	1.69	1.69	1.71
	O-H	0.97	0.97	0.97
Si_4O_4-H_2O-1	Si-O	1.73	1.73	1.75
	O-H	0.97	0.96	0.96
Si_5O_5-H_2O-1	Si-O	1.67	1.67	1.69
	O-H	0.97	0.96	0.96
Si_6O_6-H_2O-1	Si-O	1.67	1.67	1.70
	O-H	0.97	0.96	0.96
Si_7O_7-H_2O-1	Si-O	1.67	1.67	1.70
	O-H	0.97	0.96	0.96

***Table* 3.** Relative energies (kcal/mol) of the $(SiO)_n$-H_2O clusters in Models **1**, **2**, and **3**

Clusters	Model **1**	Model **2**	Model **3**
SiO-H_2O-1	0.00	0.00	0.00
SiO-H_2O-2	30.6	32.7	10.9
Si_2O_2-H_2O-1	0.00	0.00	0.00
Si_2O_2-H_2O-2	14.6	12.1	10.3
Si_3O_3-H_2O-1	0.00	0.00	0.00
Si_3O_3-H_2O-2	3.75	2.68	3.49
Si_4O_4-H_2O-1	0.00	0.00	0.00
Si_4O_4-H_2O-2	4.62	9.11	7.32
Si_5O_5-H_2O-1	0.00	0.00	0.00
Si_5O_5-H_2O-2	4.70	5.02	4.59
Si_5O_5-H_2O-3	27.6	24.8	18.6
Si_6O_6-H_2O-1	0.00	0.00	0.00
Si_6O_6-H_2O-2	3.82	3.73	2.54
Si_6O_6-H_2O-3	26.2	22.8	15.4
Si_7O_7-H_2O-1	0.00	0.00	0.00
Si_7O_7-H_2O-2	4.78	4.96	4.44
Si_7O_7-H_2O-3	43.4	54.7	48.0

of Si-O and O-H are 1.67-1.75 Å and 0.96-0.97 Å, respectively, using Models **1**, **2**, and **3** in all $(SiO)_n$-H_2O clusters with n = 1-7. The **SiO-H_2O-2** cluster was the second most stable structure, and the results revealed that an H_2O molecule was not attached to the optimized SiO cluster. The bond lengths between the Si and O atom of the H_2O molecule in the **SiO-H_2O-2** cluster were 2.44, 2.40, and 2.39 Å, in Models **1**, **2**, and **3**, respectively. *Table* 3 lists the relative energies of the $(SiO)_n$-clusters in Models **1**, **2**, and **3**, respectively. The relative energy was calculated by determining the energy difference between the most stable structural energy and an isomer energy. The relative energies of the **SiO-H_2O-2** cluster were 30.6, 32.7, and 10.9 kcal/mol in Model **1, 2, and 3**, respectively. The highest value among the relative energies of the SiO-H_2O clusters was obtained using Model **2**, and the value of the relative energy in Model **3** was extremely low (10.9 kcal/mol).

Two types of the Si_2O_2-H_2O clusters were revealed in the simulation results (*Fig*. 2). The **Si_2O_2-H_2O-1** cluster was formed via an H transfer reaction, which was similar to that for the **SiO-H_2O-1** cluster. This cluster was the most stable among the Si_2O_2-H_2O clusters. The second most stable structure was one in which the H_2O molecule did not attach to the optimized Si_2O_2 cluster (i.e., **Si_2O_2-H_2O-2** cluster). The bond lengths of Si-O between the H_2O molecule and the optimized Si_2O_2 cluster were 2.25, 2.22, and 2.22 Å in Models **1**, **2**, and **3**, respectively. The relative energies of the **Si_2O_2-H_2O-2** cluster were 14.6, 12.1, and 10.3 kcal/mol in Model **1**, **2**, and **3**, respectively. The relative energies were similar in Models **1**, **2**, and **3**.

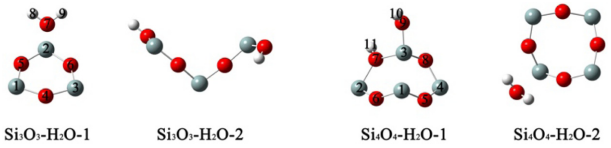

***Figure* 3.** Optimized structures of the Si_3O_3-H_2O and Si_4O_4-H_2O clusters using Model **1**. Si, O, and H atoms are denoted by gray, red, and white spheres, respectively.

Among the Si_3O_3-H_2O clusters, only two types of structures were reported following the simulations. The most stable structure was the optimized Si_3O_3 cluster with an unattached H_2O (**Si_3O_3-H_2O-1** cluster). The second most stable structure, **Si_3O_3-H_2O-2**, was a broken six-membered-ring of the optimized Si_3O_3 cluster formed by the H transfer reaction. The optimized Si_3O_3-H_2O clusters using Model **1** are shown in *Fig*. 3. Additionally, the bond lengths between the H_2O molecule (O atom (7)) and Si_3O_3 cluster (Si atom (2)) were 2.32, 2.25, and 2.22 Å in Models **1**, **2**, and **3**, respectively. The relative energies of the **Si_3O_3-H_2O-2** cluster were low at 3.75, 2.68, and 3.49 kcal/mol in Models **1**, **2**, and **3**, respectively. Notably, the order of stability of the Si_3O_3-H_2O clusters differed from that for the SiO-H_2O and Si_2O_2-H_2O clusters. Among the SiO-H_2O and Si_2O_2-H_2O clusters, the second most stable clusters were the optimized SiO and Si_2O_2 clusters with an unattached H_2O molecule.

Among the Si_4O_4-H_2O clusters, only two types of structures were simulated, and the optimized structures are shown in *Fig*. 3. The most stable structure was the **Si_4O_4-H_2O-1** cluster, which was formed by the H transfer from an H_2O molecule. The second most stable Si_4O_4-H_2O cluster (**Si_4O_4-H_2O-2**) was formed when the optimized Si_4O_4 cluster was unattached to an H_2O molecule, as shown in *Fig*. 3. The relative energies of the **Si_4O_4-H_2O-2** cluster were 4.62, 9.11, and 7.32 kcal/mol in Models **1**, **2**, and **3**, respectively. The relative energy exhibited the highest value in Model **2**.

Among the Si_5O_5-H_2O clusters, the structures with relative energies below 30 kcal/mol were in Model **1**. **Si_5O_5-H_2O-1** and **Si_5O_5-H_2O-2** structures were formed by breaking the Si(1)-Si(3) bond of the optimized Si_5O_5 cluster upon reaction with an H_2O molecule. The most stable Si_5O_5-H_2O cluster was **Si_5O_5-H_2O-1**, in which the H atom of an H_2O molecule was attached to the Si(3) atom, and the OH bond was attached to the Si(1) atom. The second most stable Si_5O_5-H_2O cluster was the opposite for the **Si_5O_5-H_2O-1**

***Figure* 4.** Optimized structures of the Si_5O_5-H_2O clusters using Model **1**. Si, O, and H atoms are denoted by gray, red, and white spheres, respectively.

***Figure* 5.** Optimized structures of the Si_6O_6-H_2O clusters using Model **1**. Si, O, and H atoms are denoted by gray, red, and white spheres, respectively.

cluster, in which the H atom and OH bond of the H_2O molecule were attached to the Si(1) and Si(3) atoms, respectively. The third most stable cluster, **Si_5O_5-H_2O-3**, did not attach to the optimized Si_5O_5 cluster or H_2O molecule. The relative energies of these clusters were 4.70 and 27.6 kcal/mol in Model **1**. The relative energies of the **Si_5O_5-H_2O-2** clusters were similar in Models **1**, **2 and 3**. Moreover, the relative energies of the **Si_5O_5-H_2O-3** clusters decreased from Model **1** to **3** (*Table* 3). The bond lengths of Si-H were 1.47, 1.47, and 1.48 Å, in Models **1**, **2**, and **3**, respectively.

Among the Si_6O_6-H_2O clusters, three optimized structures are reported in *Fig*. 5. The Si_6O_6-H_2O structures exhibited a relative energy below 30 kcal/mol in Model **1**. The most stable Si_6O_6-H_2O cluster (**Si_6O_6-H_2O-1**) was formed by an H_2O molecule attacking the Si(1)-Si(3) bond of the optimized Si_6O_6 cluster. Particularly, the OH bond and H atom of the H_2O molecule are attached to the Si(1) and Si(3) atoms, respectively. In the second most stable Si_6O_6-H_2O cluster (**Si_6O_6-H_2O-2**), the attacking position of the H_2O molecule was the same as that for the **Si_6O_6-H_2O-1** cluster. However, the positions of the OH bond and H atom of the H_2O molecule were opposite to those of the **Si_6O_6-H_2O-1** cluster. The relative energies of the **Si_6O_6-H_2O-2** cluster were 3.82, 3.73, and 2.54 kcal/mol in Models **1**, **2**, and **3**, respectively. The relative energies of the **Si_6O_6-H_2O-2** cluster were low, and no significant differences were observed between Models **1**, **2**, and **3** (*Table* 3). The third most stable Si_6O_6-H_2O cluster (**Si_6O_6-H_2O-3**), in which an H_2O molecule attached to the Si(1) atom to generate the hydrogen bonds, exhibited bond lengths of 1.82, 1.73, and 1.70 Å in Models **1**, **2**, and **3**, respectively. The relative energy of the **Si_6O_6-H_2O-3** cluster is decreased from Model **1** to **3**. Si-H bonds in the **Si_6O_6-H_2O-1** cluster exhibited bond lengths of 1.47, 1.47, and 1.48 Å in Models **1**, **2**, and **3**, respectively.

Among the Si_7O_7-H_2O clusters, the structures having less than 45 kcal/mol of relative energy were in Model **1**. The most stable and the second most stable structures were

***Table* 4.** Bader charge distributions of the $(SiO)_n$-H_2O clusters in Model **1**

Clusters	qSi(atom number)		qO(atom number)		qH(atom number)	
SiO-H_2O-1	2.09(1)		-1.61(3)		0.57(4)	0.57(5)
Si_2O_2-H_2O-1	2.12(1)	2.09(2)	-2.05(3)	-2.06(4)	0.65(6)	1.00(7)
			-1.69(5)			
Si_3O_3-H_2O-1	2.11(1)	2.11(2)	-2.09(4)	-2.09(5)	1.00(8)	0.64(9)
	2.11(3)		-2.09(6)	-1.59(7)		
Si_4O_4-H_2O-1	2.20(1)	2.11(2)	-2.07(5)	-2.09(6)	1.00(10)	1.00(11)
	2.11(3)	2.11(4)	-2.12(7)	-2.03(8)		
			-2.00(9)			
Si_5O_5-H_2O-1	2.09(1)	2.13(2)	-2.09(6)	-2.13(7)	1.00(12)	-0.96(13)
	3.89(3)	2.13(4)	-1.99(8)	-2.05(9)		
	2.11(5)		-2.08(10)	-1.99(11)		
Si_6O_6-H_2O-1	2.11(1)	2.10(2)	-2.08(7)	-1.99(8)	0.67(14)	-0.96(15)
	3.89(3)	2.13(4)	-2.07(9)	-2.15(10)		
	2.10(5)	2.13(6)	-2.22(11)	-2.06(12)		
Si_7O_7-H_2O-1	2.14(1)	2.15(2)	-2.03(8)	-2.22(9)	1.00(16)	-0.97(17)
	1.99(3)	3.88(4)	-2.14(10)	-2.05(11)		
	2.10(5)	2.03(6)	-2.21(12)	-2.00(13)		
	2.12(7)		-2.05(14)	-1.97(15)		

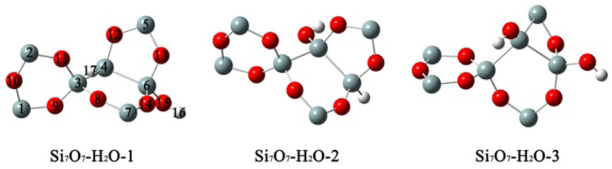

***Figure* 6.** Optimized structures of the Si_7O_7-H_2O clusters using Model **1**. Si, O, and H atoms are denoted by gray, red, and white spheres, respectively.

formed by an H_2O molecule attacking the Si(4)-Si(6) bond of the optimized Si_7O_7 cluster. Particularly, the OH bond attached to the Si(6) atom and the H atom attached to the Si(4) atom in the **Si_7O_7-H_2O-1** cluster. The **Si_7O_7-H_2O-2** cluster exhibited the opposite phenomenon. In the Si_5O_5-H_2O and Si_6O_6-H_2O clusters, the Si-Si bond broke after attacking an H_2O molecule. However, the Si(4)-S(6) bond did not break after reacting with an H_2O molecule, because two Si-Si bonds (Si(3)-Si(4)-Si(6)) were in the optimized Si_7O_7 cluster. The average Si-Si bond lengths of the **Si_7O_7-H_2O-1** cluster were 2.33, 2.33, and 2.34 Å in Models **1**, **2**, and **3**, respectively. The Si-H bond lengths were 1.48, 1.49, and 1.49 Å in Models **1**, **2**, and **3**, respectively. The relative energies of the **Si_7O_7-H_2O-2** cluster were 4.78, 4.96, and 4.44 kcal/mol in Model **1**, **2**, and **3**, respectively. The relative energies of the three chemistry models were considerably similar. The relative energies of the **Si_7O_7-H_2O-3** cluster were extremely high in the three chemistry models (*Table* 3). The most stable structures of $(SiO)_n$-H_2O with n = 1-7 clusters were formed by the H transfer from an H_2O molecule, except for the **Si_3O_3-H_2O-1** cluster.

The Bader charge distributions on the Si and O atoms of the optimized SiO and $(SiO)_n$-H_2O clusters with n = 1-7 were listed in *Tables* 1 and 4, respectively. The attachment positions of an H_2O on the SiO clusters exhibited the highest fraction of electrons. The clusters were symmetrical from SiO to Si_4O_4 clusters, and the Bader charge distributions of each Si atom were similar. Therefore, no selectivity in the reaction of the H_2O was observed. However, in the **Si_5O_5-H_2O-1**, **Si_6O_6-H_2O-1**, and **Si_7O_7-H_2O-1** clusters, the positions where the H_2O reacted contain the Si atom with the highest fraction of electrons. For instance, the Si(1)-Si(3), Si(1)-Si(3), and Si(4)-Si(6) bonds react with H_2O in the Si_5O_5, Si_6O_6, and Si_7O_7 clusters, respectively. The Bader charges of Si(1), Si(1), and Si(4) were 2.13, 2.13, and 2.60, respectively, which were the highest fraction of electrons, as shown in *Table* 1.

Fig. 7 shows the reaction energies of the SiO clusters reacting with H_2O molecules using Models **1**, **2**, and **3**. All

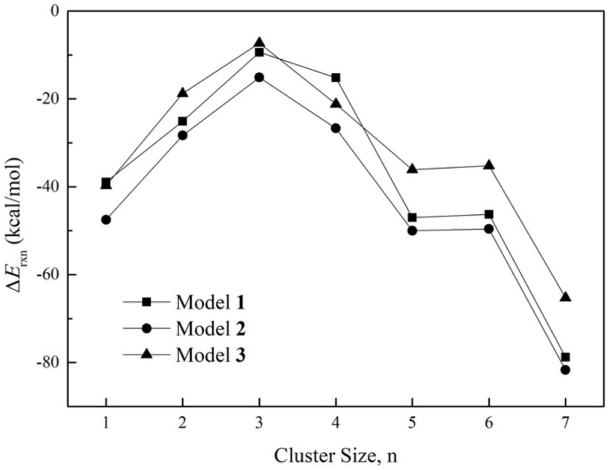

***Figure* 7.** Reaction energies (kcal/mol) of the SiO clusters with H_2O using Models **1**, **2**, and **3**.

reactions are exothermic. The three chemistry models exhibited similar patterns; thus, the reaction energies decreased from SiO to Si_3O_3 clusters and increased from Si_3O_3 to Si_7O_7 clusters. Moreover, the Si_3O_3 cluster with H_2O exhibited the lowest reaction energy among the three chemistry models because the H_2O molecule did not attach to the optimized Si_3O_3 cluster. In the future work, we will study the reaction of SiO clusters with organic compounds.

CONCLUSION

We investigated the H_2O reaction in SiO clusters using *ab initio* MC and DFT calculations. Three chemistry models were used in the study. Models **1** and **3** showed the PBE1/DGDZVP and PBE1/aug-cc-pVDZ levels of theory. Model **2** is PBE1/DGDZVP (Si atom) and aug-cc-pVDZ (O and H atoms). Two or three stable structures, with their corresponding relative energies, were reported. The reaction energies were endothermic, with the Si_3O_3-H_2O cluster exhibiting the highest values. The three chemistry models exhibited similar patterns with respect to the relative and reaction energies. Model **1** has excellent reaction energies and structural properties like Model **3**. The reaction sites of the Si_5O_5, Si_6O_6, and Si_7O_7 clusters between the H_2O and SiO clusters constituted the highest fraction of electrons from the Bader charge distributions.

Acknowledgments. This work was supported by the National Research Foundation of Korea (NRF) grant funded by the Korean government (MSIT)(NRF-2018R1D1A1-B07042931).

REFERENCES

1. Desurvire, E., *Phys. Today* **1994**, *47*, 20.
2. Kim, S.; Park, J.; Phong, P. D.; Shin, C.; Iftiquar, S. M.; Yi, J., *Sci. Rep.* **2018**, *8*, 10657.
3. Beladiya, V.; Becker, M.; Faraz, T.; Kessels, W. M. M.; Schenk, P.; Otto, F.; Fritz, T.; Gruenewald, M.; Helbing, C.; Jandt, K. D.; Tünnermann, A.; Sierka, M.; Szeghalmi, A., *Nanoscale* **2020**, *12*, 2089.
4. Liu, Z.; Yu, Q.; Zhao, Y.; He, R.; Xu, M.; Feng, S.; Li, S.; Zhou, L.; Mai, L., *Chem. Soc. Rev.* **2019**, *48*, 285.
5. Bitar, A.; Ahmad, N. M.; Fessi, H.; Elaissari, A., *Drug Discov. Today* **2012**, *17*, 1147.
6. Bergeron, D. E.; Jr., A. W. C., *J. Chem. Phys.* **2002**, *117*, 3219.
7. Torres, R.; Martin, M., *Appl. Surf. Sci.* **2002**, *193*, 149.
8. Nath, K. G.; Shimoyama, I.; Sekiguchi, T.; Baba, Y., *Appl. Surf. Sci.* **2004**, *234*, 234.
9. Mehner, T.; Göcke, H. J.; Schunck, S.; Schnöckel, H., *Z. Anorg. Allg. Chem.* **1990**, *580*, 121.
10. Nayak, S. K.; Rao, B. K.; Khanna, S. N.; Jena, P., *J. Chem. Phys.* **1998**, *109*, 1245.
11. Chu, T. S.; Zhang, R. Q.; Cheung, H. F., *J. Phys. Chem. B* **2001**, *105*, 1705.
12. Lu, W. C.; Wang, C. Z.; Nguyen, V.; Schmidt, M. W.; Gordon, M. S.; Ho, K. M., *J. Phys. Chem. A* **2003**, *107*, 6936.
13. Hu, S.-X.; Yu, J.-G.; Zeng, E. Y., *J. Phys. Chem. A* **2010**, *114*, 10769.
14. Byun, H.-G.; Kim, I.; Kwon, H.-S.; Bae, G.-T., *Bull. Korean Chem. Soc.* **2017**, *38*, 1310.
15. Bae, G.-T., *Bull. Korean Chem. Soc.* **2019**, *40*, 780.
16. Godbout, N.; Salahub, D. R.; Andzelm, J.; Wimmer, E., *Can. J. Chem.* **1992**, *70*, 560.
17. Sosa, C.; Andzelm, J.; Elkin, B. C.; Wimmer, E.; Dobbs, K. D.; Dixon, D. A., *J. Phys. Chem.* **1992**, *96*, 6630.
18. Dunning, T. H., Jr., *J. Chem. Phys.* **1989**, *90*, 1007.
19. Kendall, R. A.; Dunning, T. H., Jr.; Harrison, R. J., *J. Chem. Phys.* **1992**, *96*, 6796.
20. Woon, D. E.; Dunning, T. H., Jr., *J. Chem. Phys.* **1993**, *98*, 1358.
21. Peterson, K. A.; Woon, D. E.; Dunning, T. H., Jr., *J. Chem. Phys.* **1994**, *100*, 7410.
22. Wilson, A. K.; van Mourik, T.; Dunning, T. H., *J. Mol. Struct.: THEOCHEM* **1996**, *388*, 339.
23. Li, S.; Hennigan, J. M.; Dixon, D. A.; Peterson, K. A., *J. Phys. Chem. A* **2009**, *113*, 7861.
24. Shi, B.; Weissman, S.; Bruneval, F.; Kronik, L.; Öğüt, S., *J. Chem. Phys.* **2018**, *149*, 064306.
25. Frisch, M. J.; Trucks, G. W.; Schlegel, H. B.; Scuseria, G. E.; Robb, M. A.; Cheeseman, J. R.; Scalmani, G.; Barone, V.; Mennucci, B.; Petersson, G. A.; Nakatsuji, H.; Caricato, M.; Li, X.; Hratchian, H. P.; Izmaylov, A. F.; Bloino, J.; Zheng, G.; Sonnenberg, J. L.; Hada, M.; Ehara, M.; Toyota, K.; Fukuda, R.; Hasegawa, J.; Ishida, M.; Nakajima, T.; Honda, Y.; Kitao, O.; Nakai, H.; Vreven, T.; Montgomery Jr., J. A.; Peralta, J. E.; Ogliaro, F.; Bearpark, M. J.; Heyd, J.; Brothers, E. N.; Kudin, K. N.; Staroverov, V. N.; Kobayashi, R.; Normand, J.; Raghavachari, K.; Rendell, A. P.; Burant, J. C.; Iyengar, S. S.; Tomasi, J.; Cossi, M.; Rega, N.; Millam, N. J.; Klene, M.; Knox, J. E.; Cross, J. B.; Bakken, V.; Adamo, C.; Jaramillo, J.; Gomperts, R.; Stratmann, R. E.; Yazyev, O.; Austin, A. J.; Cammi, R.; Pomelli, C.; Ochterski, J. W.; Martin, R. L.; Morokuma, K.; Zakrzewski, V. G.; Voth, G. A.; Salvador, P.; Dannenberg, J. J.; Dapprich, S.; Daniels, A. D.; Farkas, Ö.; Foresman, J. B.; Ortiz, J. V.; Cioslowski, J.; Fox, D. J., *Gaussian 09*. Gaussian, Inc.: Wallingford, CT, USA, 2009.
26. Bae, G.-T.; Dellinger, B.; Hall, R. W., *J. Phys. Chem. A* **2011**, *115*, 2087.
27. Bae, G.-T., *Bull. Korean Chem. Soc.* **2016**, *37*, 638.
28. Bae, G.-T., *Struct. Chem.* **2021**, *32*, 1787.
29. Henkelman, G.; Arnaldsson, A.; Jónsson, H., *Comput. Mater. Sci.* **2006**, *36*, 354.